Non-equilibrium crystalline phases formed in the Co-Ta system by ion beam mixing

1994 J. Phys.: Condens. Matter 6 9065

(http://iopscience.iop.org/0953-8984/6/43/011)

J. Phys.: Condens. Matter 6 (1994) 9065–9074. Printed in the UK

Non-equilibrium crystalline phases formed in the Co–Ta system by ion beam mixing

Z J Zhang†‡ and B X Liu†‡

† Department of Materials Science and Engineering, Tsinghua University, Beijing 100084, People's Republic of China

‡ Center of Condensed Matter and Radiation Physics, China Center of Advanced Science and Technology (World Laboratory), Beijing 100080, People's Republic of China

Received 12 April 1994, in final form 18 May 1994

Abstract. Co-rich Co–Ta solid solutions of the high-temperature Co FCC structure were synthesized by 200 keV room-temperature xenon ion mixing. The experimental results revealed that these FCC solid solutions were formed gradually from the Co hexagonal solid solutions through a HCP → FCC transition, that the solid solubility was greatly beyond the equilibrium value up to 20 at.% Ta, and that their lattice parameters followed the prediction of Vegard's law. Interestingly, a new metastable crystalline phase of FCC structure with $a = 4.43$ Å was formed in two Ta-rich films, i.e. $Co_{30}Ta_{70}$ and $Co_{25}Ta_{75}$ multilayered films, at different irradiation stages. The thermal stabilities of the Co-rich and the Ta-rich metastable crystalline phases were also studied by thermal annealing.

1. Introduction

In the past 10 years, ion beam mixing (IM) has proved to be a powerful means of synthesizing a variety of metastable alloys with an amorphous or a crystalline structure in about 70 binary metal systems [1–3]. On the basis of these studies, the glass-forming ability of the binary metal systems was found to extend much more broadly than predicted according to the results obtained by the liquid-melt-quenching technique. Concerning the formation of the metastable crystalline (MX) phases by ion mixing, many supersaturated solid solutions have been formed, which always have the same crystalline structure as that of the major alloying elements of their room-temperature (RT) structures [4], even though in some cases the elements have another structure at high temperatures. Very recently, however, a new FCC MX phase was observed by the present authors' group in three Nb-based BCC binary systems by IM and was formed via a two-step BCC → HCP → FCC transition [5]. It is therefore of interest to study further this type of MX phase in the binary systems of BCC metal type, e.g. in the Ta-based BCC systems. It is also of interest to study the possibility of forming supersaturated solid solutions of high-temperature structures by IM, e.g. cobalt-rich phases, which have two different structures, namely HCP and FCC phases, at low and high temperatures, respectively. The Ta–Co system was therefore chosen for this study. In the Co–Ta equilibrium phase diagram, there are two solid solutions based on cobalt. One is of HCP structure and is stable at RT. The other is of FCC structure and stable at temperatures higher than 400 °C. The equilibrium solid solubility of the two Co-based solid solutions of different structures is only several atomic per cent of Ta. We present, in this paper, our results on the formation and the relevant mechanisms of the new MX phases observed in both the Ta-rich BCC and the Co-rich HCP ranges by ion irradiation.

0953-8984/94/439065+10$19.50

2. Experimental procedure

Multilayered Co–Ta films were prepared by vapour deposition of pure (99.99%) cobalt and pure (99.9%) tantalum onto cleaved NaCl single crystals as substrates in a vacuum evaporation system whose background vacuum level was of the order of 10^{-7} Torr. The total thickness of the films was designed to match the projected range plus the projected range straggling of the irradiation ions, i.e. 400 Å for 200 keV xenon ions. Usually five to eight layers were deposited for one sample. The composition of the films was controlled by adjusting the relative thickness of the two constituent metals and was later determined by energy-dispersive spectroscopy (EDS) analysis. The as-deposited Co–Ta films were then irradiated with 200 keV xenon ions to doses ranging from 3×10^{14} to 1×10^{16} Xe^+ cm^{-2} at RT. During irradiation, the beam current density of the high-energy xenon ions was controlled to be less than 1 μA cm^{-2} to minimize the beam-heating effect, and the temperature of the substrates was estimated to be around 100–150 °C. After irradiation, all the mixed samples were analysed by transmission electron microscopy (TEM) observation and selected-area diffraction (SAD) analysis to identify the structures of the resultant phases. Meanwhile, EDS analysis was employed to determine the actual composition of the formed phases. To evaluate the thermal stability of the mixed phases, thermal annealing experiments of the corresponding films were carried out *in situ* in the hot stage attached to the transmission electron microscope, where the vacuum level was of the order of 10^{-7} Torr.

3. Results and discussion

3.1. Formation of Co-rich FCC solid solution

Table 1 lists the structural changes of the $Co_{98}Ta_2$, $Co_{93}Ta_7$, $Co_{86}Ta_{14}$ and $Co_{80}Ta_{20}$ multilayered films induced by RT 200 keV xenon ion mixing, when the irradiation dosages were increased. The compositions of the above-mentioned multilayered films were all determined by EDS analysis, for which the error was within 5%. Figures 1(*a*) and (*b*) are the EDS analysis results of one sample with a Co:Ta stoichiometry of 80:20 before and after ion mixing. From table 1, it is obvious that in the four Co-rich samples, i.e. in $Co_{98}Ta_2$, $Co_{93}Ta_7$, $Co_{86}Ta_{14}$ and $Co_{80}Ta_{20}$ films, a structural HCP → FCC transition was induced gradually on irradiation with high-energy xenon ions. If we take the HCP → FCC transition in the $Co_{98}Ta_2$ film as an example, figure 2(*a*) shows a bright-field image of the as-deposited $Co_{98}Ta_2$ films. When the film was irradiated to relatively low doses, i.e. $(3–7) \times 10^{14}$ Xe^+ cm^{-2}, the structures of the films were hexagonal, indicating the formation of a solid solution based on the hexagonal cobalt. Figure 2(*b*) shows a SAD pattern of the Co-based hexagonal solid solution, in which the diffraction lines from the BCC Ta were invisible. When the irradiation dose was increased to 9×10^{14} Xe^+ cm^{-2}, some new diffraction lines emerged in the SAD pattern of the $Co_{98}Ta_2$ film, coexisting with those from the hexagonal solid solution. This suggested that a new crystalline phase nucleated and grew from the matrix of the Co-rich hexagonal solid solution. Figure 2(*c*) shows a SAD pattern of the $Co_{98}Ta_2$ film at this irradiation stage. When the irradiation dose was further increased to 3×10^{15} Xe^+ cm^{-2}, all the diffraction lines from the Co-rich hexagonal solid solution disappeared, leaving only the newly emerged diffraction lines in the SAD pattern shown by figure 2(*d*), which suggested that the transition from the Co-rich hexagonal solid solution to a new crystalline phase was fulfilled. These newly emerged diffraction lines were identified to be from a FCC phase with the lattice parameter being 3.55 Å, which was listed in the last row of table 1. The error in the lattice parameters determined by SAD was

less than 2% for all samples. The lattice parameter of the FCC phase, i.e. 3.55 Å, matched well that of the high-temperature Co FCC phase, i.e. $a = 3.552$ Å, and thus the newly formed FCC phase was a Co-rich solid solution of the high-temperature Co FCC structure. In other words, the observed structural HCP $\rightarrow$ FCC transition in the $Co_{98}Ta_2$ film was actually a phase transition from Co-based hexagonal to Co-based FCC solid solution. In other Co-rich samples, i.e. the $Co_{93}Ta_7$, $Co_{86}Ta_{14}$ and $Co_{80}Ta_{20}$ multilayered films, the same HCP $\rightarrow$ FCC transition was also observed at the respective irradiation stages. The lattice parameters of these high-temperature FCC solid solutions obtained in the Co-rich samples were 3.57 Å, 3.60 Å and 3.65 Å, respectively (see table 1). An interesting point here is that the Co-based FCC solid solutions, which are only obtainable at temperatures higher than 400 °C by traditional materials processing, were synthesized at RT IM though the effective temperature of the films during IM was estimated to be around 100–150 °C, which was still considerably lower than 400 °C.

Table 1. Formation of the Co-rich FCC solid solutions under RT 200 keV xenon IM. HCP stands for the Co-rich HCP solid solution, and FCC the Co-rich FCC solid solution.

Irradiation dose (10^{14})	Phases formed			
	$Co_{98}Ta_2$	$Co_{93}Ta_7$	$Co_{86}Ta_{14}$	$Co_{80}Ta_{20}$
3	HCP	HCP	HCP	HCP
7	HCP	HCP	HCP+FCC	HCP+FCC
9	HCP+FCC	HCP+FCC	HCP+FCC	HCP+FCC
30	FCC	FCC	—	—
50	FCC	FCC	FCC	FCC
70	—	—	FCC	FCC
100	FCC	FCC	FCC	FCC
Lattice parameter (Å)	3.55 ± 0.07	3.57 ± 0.07	3.60 ± 0.07	3.65 ± 0.07

The next issue is how the Co-rich FCC solid solution was formed by RT IM. IM is commonly accepted as a far-from-equilibrium process and can be separated into two stages, i.e. the first atomic collision cascade and a subsequent relaxation period, which lasts for only 10^{-10}–10^{-9} s [6]. The structure of an alloy is believed to be formed within the relaxation period where an effective cooling speed of 10^{13}–10^{14} K s^{-1} is estimated from a thermal spike model [6]. Apparently, the kinetic condition for a new phase to grow is very restricted, which allows only either amorphous or simple structured crystalline phases to be formed [7]. As a result, only fast and partitionless transition mechanisms can proceed under IM, e.g. changing the sequence of stacking order [8], martensitic shearing or its reverse form [5]. In short, the structural compatibility between the newly formed phase and the matrix plays a major role in the crystal-to-crystal transition owing to the prohibition of long-range diffusion [5]. The above-mentioned HCP $\rightarrow$ FCC transition in the Co-rich Co–Ta films is a fast transition mechanism and can be easily accomplished through an atomic stacking order change, i.e. through a sliding of the atoms on the $\{0002\}_{HCP}$ plane along the $\langle 1\bar{1}00\rangle_{HCP}$ direction by a vector of $\frac{1}{3}\langle 1\bar{1}00\rangle_{HCP}$, which can be realized within the very short relaxation period. Further study revealed that the lattice parameters of the FCC solid solutions were positively related to their compositions; that is, the higher the tantalum concentration, the larger is the lattice parameter. As the tantalum atom is larger than the cobalt atom, the inclusion of tantalum atoms into the cobalt lattice enlarged the lattice parameter. Figure 3 illustrates the lattice parameters of the solid solutions versus the alloy

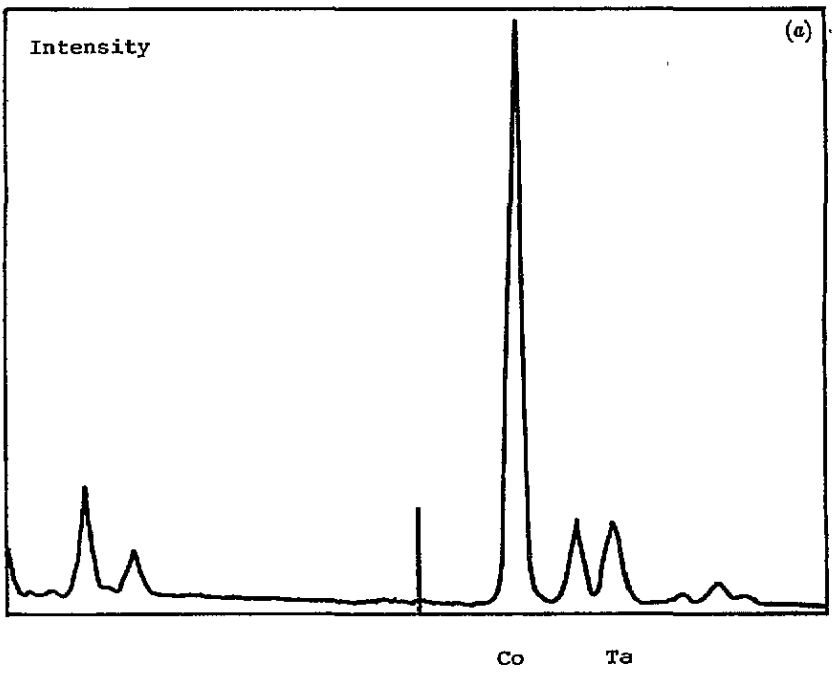

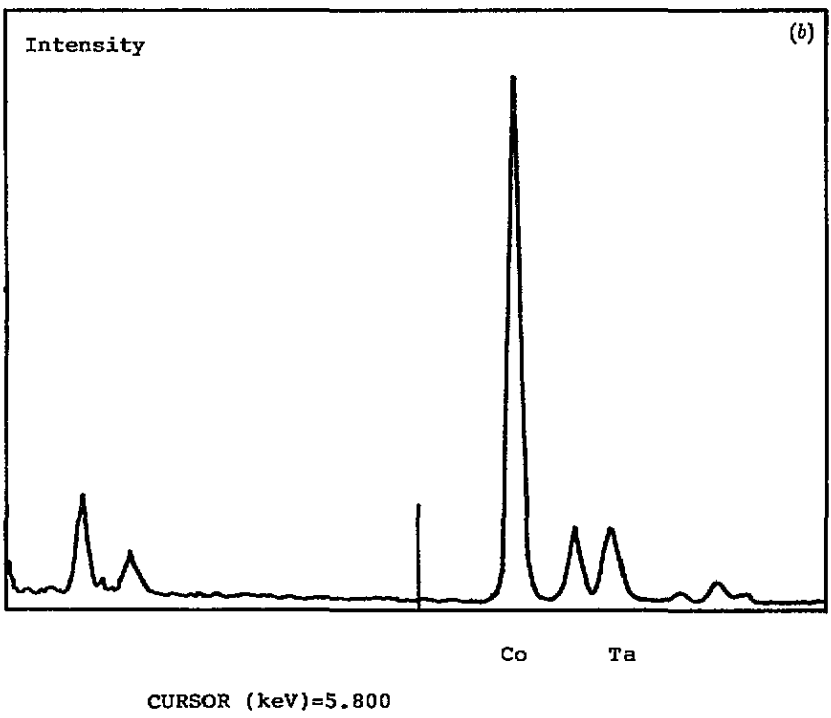

Figure 1. EDS analysis results of the $Co_{80}Ta_{20}$ films (*a*) before IM and (*b*) after 200 keV RT xenon IM to a dose of 5×10^{15} Xe^+ cm^{-2}.

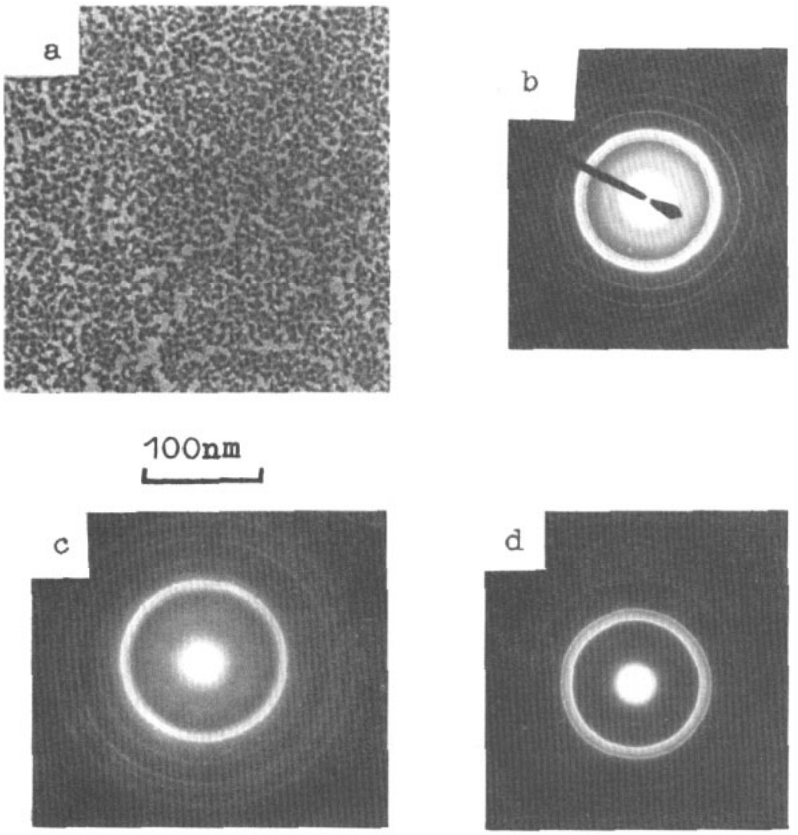

Figure 2. (*a*) Morphology of an as-deposited $Co_{98}Ta_2$ multilayered film; (*b*) SAD pattern of the Co-based hexagonal solid solution formed at a dose of 7×10^{14} Xe^+ cm^{-2}; (*c*) SAD pattern of the mixture of the Co-based hexagonal and FCC solid solutions at a dose of 9×10^{14} Xe^+ cm^{-2}; (*d*) SAD pattern of the film at a dose of 3×10^{15} Xe^+ cm^{-2}, exhibiting formation of the FCC solid solution.

compositions, from which an approximately positive linear correlation is observed. As a comparison, the prediction of the corresponding lattice parameters by a hard-sphere model [9] is also drawn in figure 3. Obviously, the predictions by the hard-sphere model agree well with the experimental values. Figure 4 shows a plot of the average atomic volume of the FCC supersaturated solid solution, calculated from the experimental values of the lattice parameters, as a function of composition. An obvious negative deviation from Vegard's law for ideal solid solutions, up to about 4%, is observed. This is qualitatively consistent with the negative heat of formation of the system [10].

3.2. Formation of Ta-rich FCC MX phase

For the Ta-rich samples, the $Co_{25}Ta_{75}$ multilayered film was completely amorphized at an irradiation dose of 1×10^{15} Xe^+ cm^{-2}. Figure 5(*a*) shows a SAD pattern of the amorphized film, where only broad haloes are exhibited. When the irradiation dose was increased to 5×10^{15} Xe^+ cm^{-2}, the amorphized $Co_{25}Ta_{75}$ multilayers changed into a FCC structure

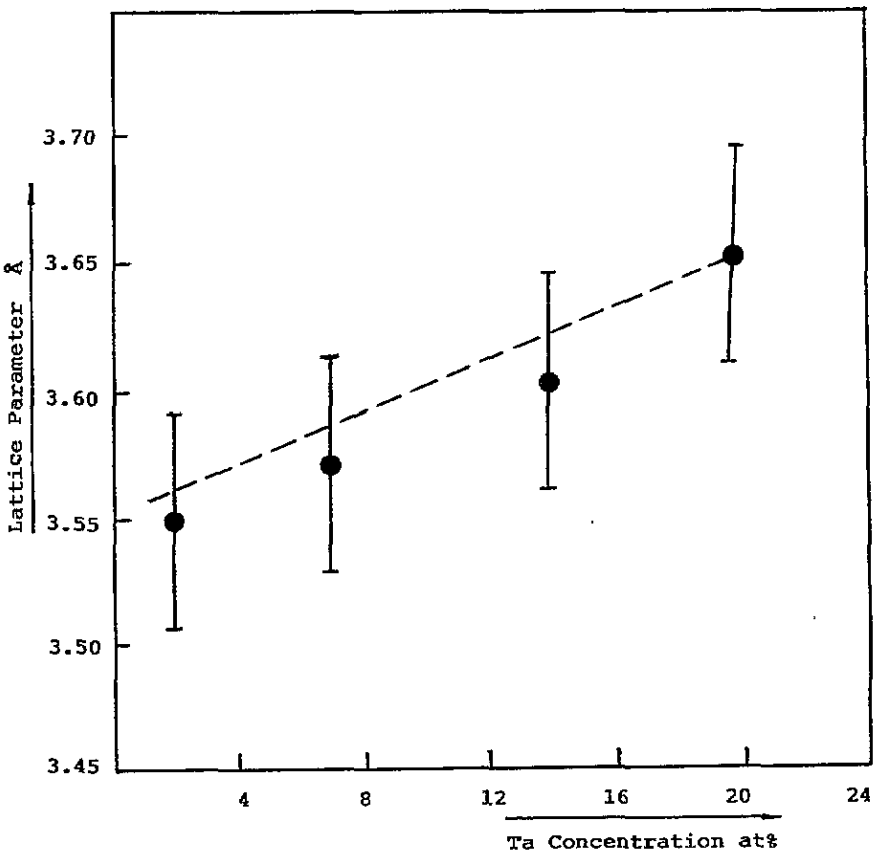

Figure 3. Relationship between the lattice parameter and composition of the FCC supersaturated solid solutions: ----, calculated from the hard-sphere model; ●, experimental values.

with a lattice parameter a of 4.43 Å. Figure 5(b) shows its SAD pattern. Table 2 is the indexing results of the FCC phase. The FCC MX phase remained unchanged upon further irradiation even to a dose as high as 1×10^{16} Xe^+ cm^{-2}. The phase transition in the $Co_{25}Ta_{75}$ multilayers under IM can thus be summarized as

$$Co_{25}Ta_{75} \xrightarrow[RT]{1\times10^{15}\ Xe^+\ cm^{-2}} \text{amorphous} \xrightarrow[RT]{5\times10^{15}\ Xe^+\ cm^{-2}} \text{FCC}. \tag{1}$$

Note that FCC is the newly formed Ta-rich MX phase. In another Ta-rich samples, i.e. a $Co_{30}Ta_{70}$ multilayered film, however, the same FCC phase was formed at a dose of 7×10^{14} Xe^+ cm^{-2} and turned amorphous at a higher dose of 5×10^{15} Xe^+ cm^{-2}. Similarly, it can be summarized as follows:

$$Co_{30}Ta_{70} \xrightarrow[RT]{7\times10^{14}\ Xe^+\ cm^{-2}} \text{FCC} \xrightarrow[RT]{5\times10^{15}\ Xe^+\ cm^{-2}} \text{amorphous}. \tag{2}$$

It should be emphasized that the FCC MX phase was formed in two Ta-rich samples, i.e. $Co_{25}Ta_{75}$ and $Co_{30}Ta_{70}$ multilayers, and yet in a reverse sequence versus the amorphous phase. The reverse formation sequence was ascribed to a little compositional difference, i.e.

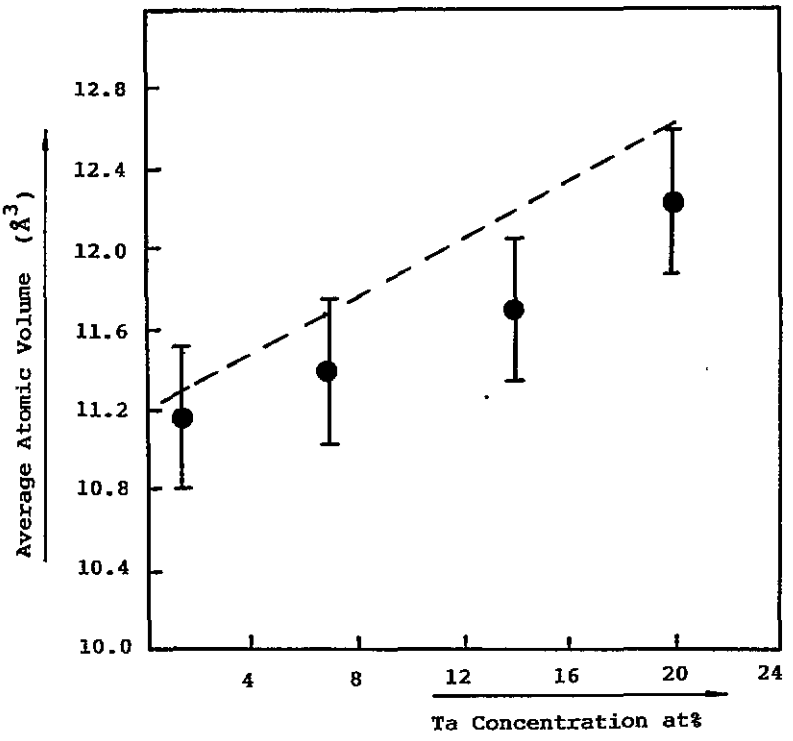

Figure 4. Average atomic volume as a function of Ta concentration, calculated from lattice parameters determined from the SAD data: ●, experimental values; ----, calculated from Vegard's law.

only 5 at.% Ta, between the two samples. In other words, the formation of the FCC MX phase was quite susceptible to the composition and can thus be considered as a linear compound [11]. By considering the Ta-rich FCC MX phase as compound like, and by using the method suggested in [11], for which the details can be found in the well documented literature [12], the free-energy curve of the FCC MX phase can be calculated and was included in the energy diagram, which can explain the above phase formation results well and will be published elsewhere soon.

3.3. Thermal stability of the Co-rich and Ta-rich MX phase

The Co-rich FCC solid solutions were quite stable under thermal annealing and remained the structure observed up to 400 °C. Upon further annealing at successively higher temperatures, however, the $Co_{98}Ta_2$ and $Co_{93}Ta_7$ FCC solid solutions remained of FCC structure at 800 °C for 1 h, while the $Co_{86}Ta_{14}$ and $Co_{80}Ta_{20}$ solid solutions turned into a mixture as shown in figure 6, which consisted of a solid solution based on FCC Co and the Ta-rich FCC MX phase, when the temperature reached 600 °C for about 1 h. This suggested that the phase separation in the $Co_{86}Ta_{14}$ and $Co_{80}Ta_{20}$ solid solutions by thermal activation should be ascribed to the superinclusion of Ta atoms into the cobalt lattice, as the lattice distortion caused by Ta atoms elevated the solid solutions to a higher-energy state than the mixture, which relaxed to a lower-energy state corresponding to the mixture upon thermal annealing. In the $Co_{25}Ta_{75}$ sample, the Ta-rich FCC MX phase remained the structure observed up to 600 °C while, in the $Co_{30}Ta_{70}$ film, it turned into a mixture similar to that shown in figure 6.

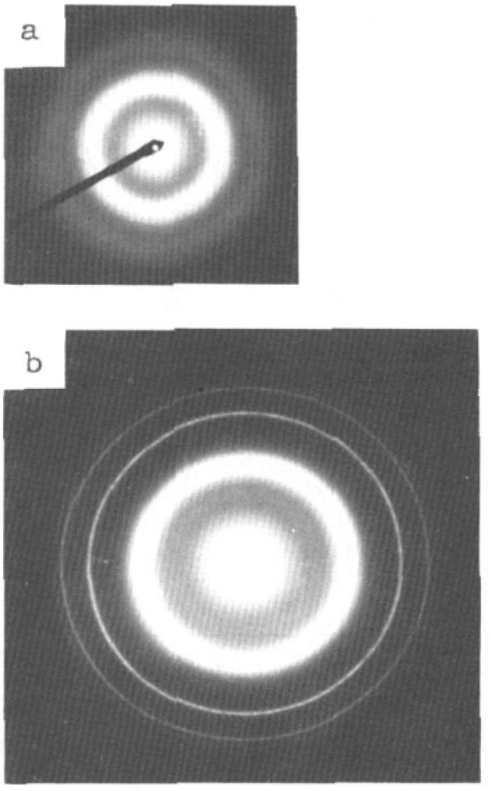

Figure 5. (*a*) SAD pattern of amorphized $Co_{25}Ta_{75}$ film at an irradiation dose of 1×10^{15} Xe^+ cm^{-2}; (*b*) SAD pattern of the Ta-rich FCC MX phase formed in the $Co_{25}Ta_{75}$ film when it was further irradiated to 5×10^{15} Xe^+ cm^{-2}.

Table 2. Identification of the FCC MX phase formed in the $Co_{25}Ta_{75}$ multilayered films by RT 200 keV xenon IM to a dose of 5×10^{15} Xe^+ cm^{-2}.

Planar spacing (experimental) (Å)	Indexing results	Planar spacing (calculation) (Å)	Intensity of lines
2.55 ± 0.05	111	2.56	Strong
2.20 ± 0.04	200	2.22	Strong
1.58 ± 0.03	220	1.57	Strong
1.34 ± 0.03	311	1.34	Strong
1.29 ± 0.03	222	1.28	Medium
1.11 ± 0.02	400	1.11	Medium
1.02 ± 0.02	331	1.02	Medium

This result supports indirectly that the FCC MX phase is sensitive to the composition and the compound-like assumption in the free-energy calculation.

4. Concluding remarks

(1) A series of Co-based FCC solid solutions were formed by 200 keV RT xenon IM

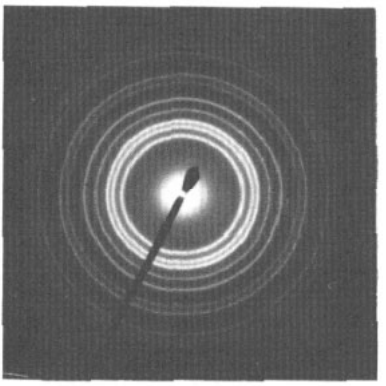

Figure 6. SAD pattern formed when the $Co_{86}Ta_{14}$ and $Co_{80}Ta_{20}$ solid solutions of high-temperature Co FCC structure were annealed at 600 °C for 1 h, showing a mixture composed of a FCC solid solution plus the quite stable Ta-rich FCC MX phase.

through a transition from the Co-based hexagonal solid solutions into the high-temperature FCC structure. The effective temperature of the samples during ion irradiation was estimated to be below 150 °C, which was considerably lower than the polymeric transition temperature of Co at 400 °C.

(2) The maximum solid solubility of the Co-based FCC solid solutions was about 20 at.% Ta and was greatly beyond the equilibrium value. The lattice parameters of the solid solutions were consistent with the prediction of Vegard's law.

(3) A new FCC phase was observed in two Ta-rich samples, i.e. $Co_{25}Ta_{75}$ and $Co_{30}Ta_{70}$ films. The FCC phase was compound like and its formation was susceptible to the composition.

Acknowledgments

This project is supported in part by the National Natural Science Foundation of China and the Fundamental Research Foundation of Tsinghua University. The authors are grateful to the staff of the Transmission Electron Microscopy Laboratory at Peking University for their help.

References

[1] Kung K T Y, Liu B X and Nicolet M A 1983 *Phys. Status Solidi* a **77** K77
[2] Liu B X, Che D Z, Zhang Z J, Lai S L and Ding J R 1991 *Phys. Status Solidi* a **128** 345
[3] Liu B X, Nicolet M A and Lau S S 1983 *Phys. Status Solidi* a **73** 183
[4] Tsaur B Y, Lau S S, Hung L S and Mayer J W 1981 *Nucl. Instrum. Methods* **182–3** 67
[5] Liu B X and Zhang Z J 1994 *J. Mater. Res.* **9** 375
[6] Thompson M V 1969 *Defects and Radiation Damage in Metals* (Cambridge: Cambridge University Press) chs 4 and 5
[7] Liu B X 1986 *Phys. Status Solidi* a **94** 11
[8] Liu B X and Zhang Z J 1994 *Phys. Rev.* B **49** 12519
[9] Zhang Z J and Liu B X 1994 *J. Phys.: Condens. Matter* **6** 2647
[10] Swalin R A 1962 *Thermodynamics of Solids* (New York: Wiley) pp 91–108

[11] Gallego L J, Somozar J A, Pernandez H M and Alonso J A 1992 *Ordering and Disordering in Alloys* ed A R Yavari (Amsterdam: Elsevier) p 328
[12] Zhang Z J, Bai H Y, Qiu Q L, Yang T, Tao K and Liu B X 1993 *J. Appl. Phys.* **73** 1702